

Supporting info

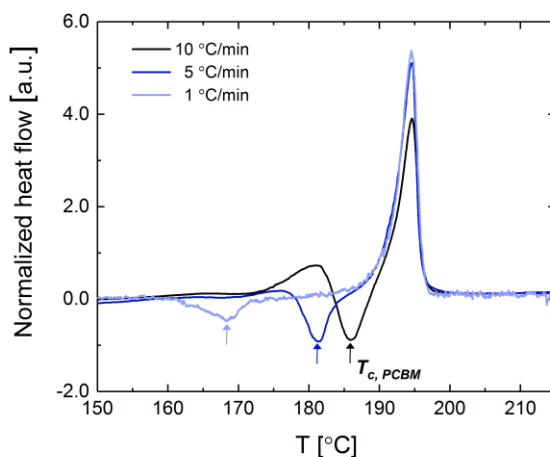


Figure S1. Typical 1st heat DSC traces for a 50:50 blend of BQR:PC₇₁BM heated at 10 °C/min, 5 °C/min, and 1 °C/min. Heat flow is normalized by sample mass m and heating rate $\beta = 10$ °C/min. Exotherm direction is down.

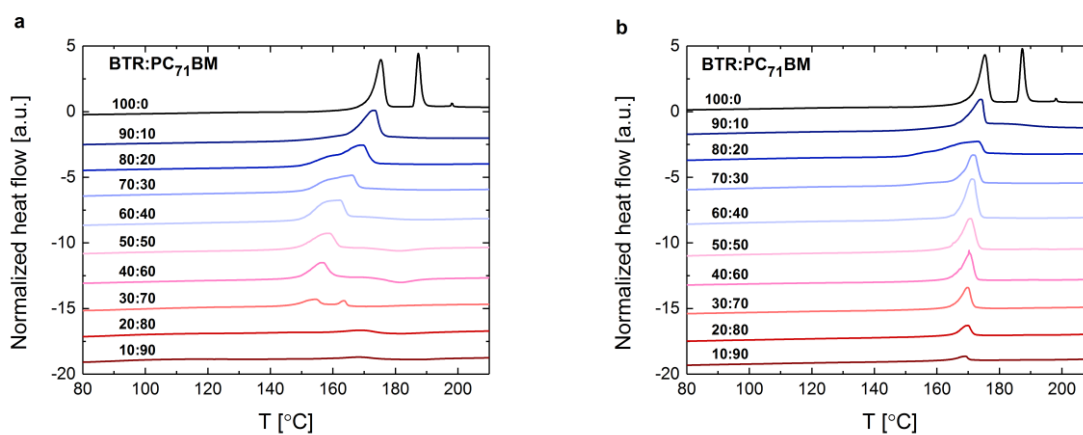


Figure S2. Typical DSC heating traces for BTR:PC₇₁BM (a) on 1st heat (as-cast morphology) and (b) on 2nd heat. Heat flow is normalized by sample mass m and heating rate $\beta = 10$ °C/min. Exotherm direction is down.

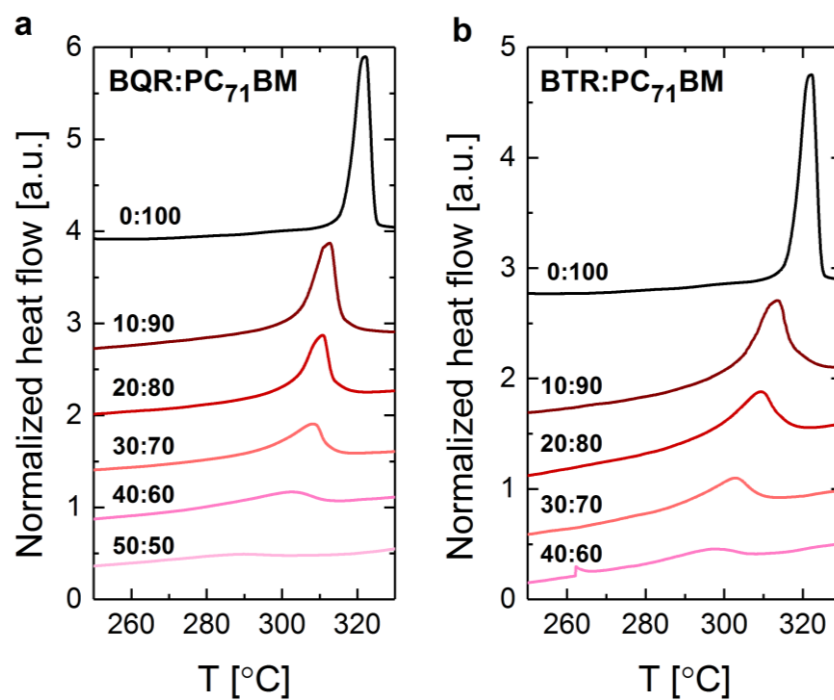


Figure S3. Typical DSC heating traces for PC₇₁BM melting in (a) BQR:PC₇₁BM and (b) BTR:PC₇₁BM blends. Heat flow is normalized by sample mass m and cooling rate $\beta = 10$ °C/min. Exotherm direction is down.

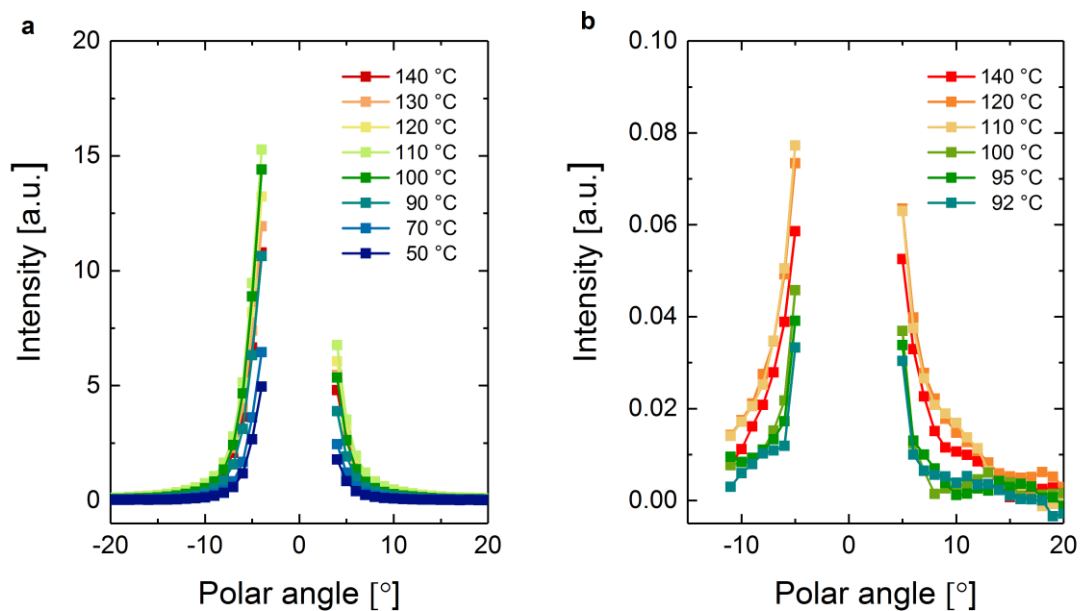


Figure S4. Extracted pole figures around (a) the primary peak ($|q| \approx 0.35 \text{ \AA}^{-1}$) and (b) the secondary peak ($|q| \approx 0.7 \text{ \AA}^{-1}$) in the GIWAXS pattern as a function of temperature upon cooling the BQR crystal at $10 \text{ }^\circ\text{C}/\text{min}$.

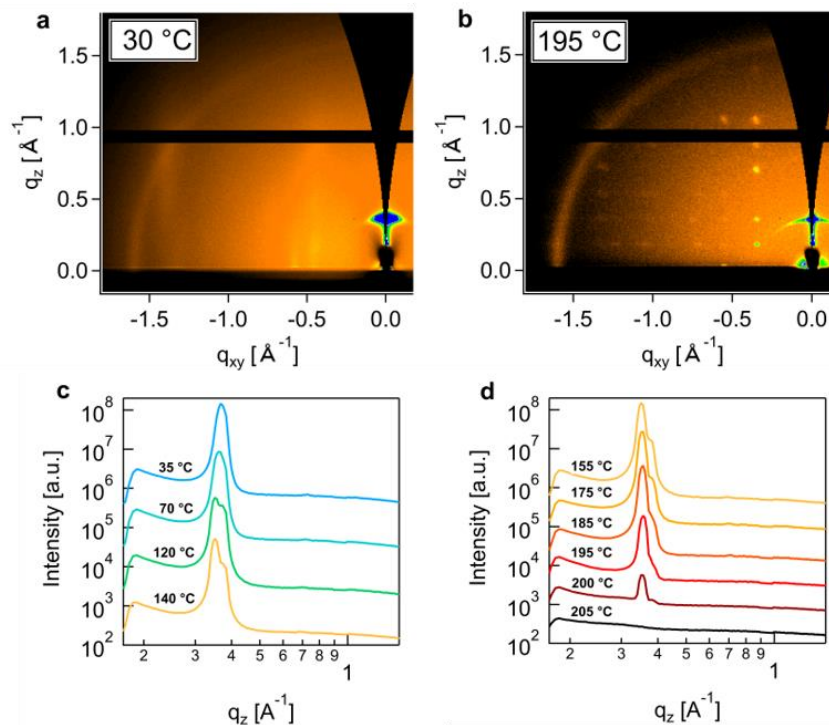


Figure S5. (a-b) GIWAXS detector images of a pristine BQR thin film blade-coated from toluene solution and annealed to the temperature specified in the figure. The images were collected while heating at 10 °C/min. (c-d) Vertical line profiles near $q_{xy} \approx 0$ are also provided.

Unit cell prediction

Upon reheating, the quiescently-cooled, pristine BQR exhibits signs of enhanced alignment indicated by sharper and more numerous high index reflections in the GIWAXS pattern. The unit cell lattice parameters for BQR were estimated from an annealed sample, reheated to 150 °C, using the Diffraction Pattern Calculator (DPC) toolkit¹ to best match the GIWAXS pattern. The contrast in the detector image and feature detection limits were adjusted manually to selectively identify relevant peaks from the local background intensity. Additionally, the extraneous intensity from main-beam bleeding over the beam stop was masked. The resulting experimental diffraction

pattern is reproduced in Figure S6a. The DPC software produces a prediction for the lattice constants by optimizing the convergence of this experimental diffraction pattern with a calculated diffraction pattern. Figure S6b displays the theoretical GIWAXS pattern at optimum convergence with the experimental scattering pattern from pristine BQR; the predicted crystal unit cell constants are reproduced in Table S1. The DPC algorithm assumes a preferred crystallite orientation in the thin film sample from which the GIWAXS data is collected and must be specified *a priori* as input to the prediction. The unit cell prediction for BQR assumes crystallites are oriented with their (010) plane parallel to the substrate. This orientation is consistent with other conjugated, organic molecules in an “edge-on” crystallite orientation;² typically the (010) plane bisects the direction of π -stacking between molecular backbones exposing the alkyl side-chains at the (010) interface, which lies parallel to the substrate.

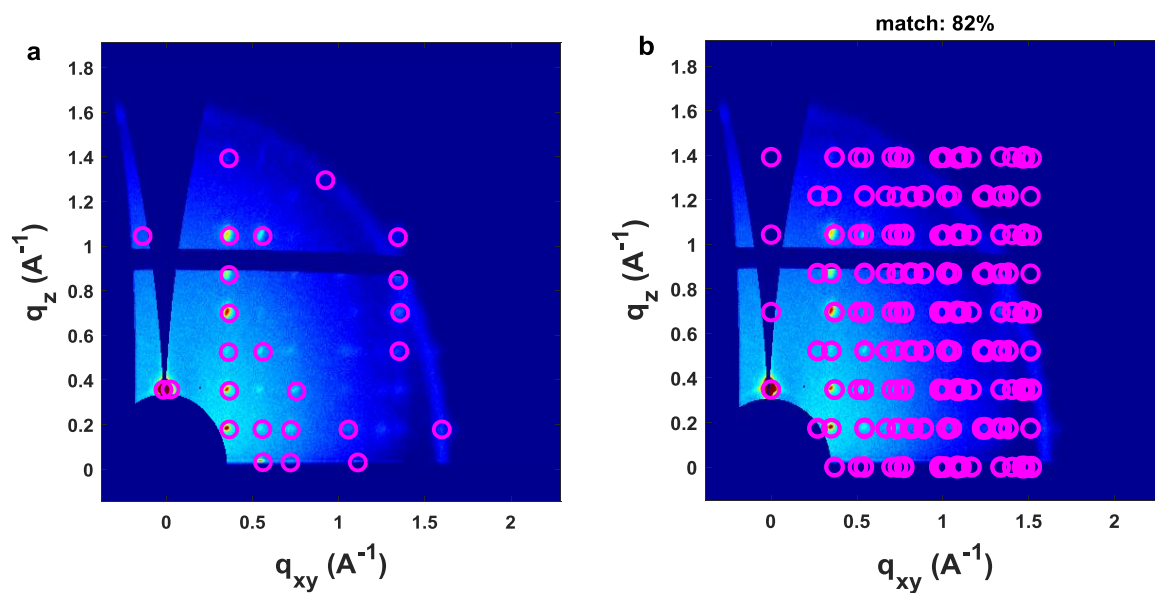


Figure S6. Experimental GIWAXS pattern for BQR that has been melted, recrystallized and reheated to 150 °C. (a) Diffraction peaks are identified from the signal background by

overlapping circles using the DPC toolkit. (b) The predicted scattering pattern for the crystal unit cell of BQR, reproduced in Table 1, with the (010) plane in contact with the surface is shown.

Table S1. Unit cell lattice parameters for BTR, previously determined by single crystal diffraction,³ and BQR, predicted from the GIWAXS pattern assuming the (010) plane is parallel to the substrate. The sample temperature at which the measurement was performed is indicated.

Unit cell parameters	BTR³	BQR
<i>T</i>	-173 °C	150 °C
<i>a</i>	14.257 Å	19 Å
<i>b</i>	20.519 Å	22 Å
<i>c</i>	21.795 Å	24 Å
<i>α</i>	114.76 °	115 °
<i>β</i>	98.08 °	108 °
<i>γ</i>	102.00 °	105 °

It is important to note that the lattice constants for BQR in Table 1 do not constitute a unique solution for the unit cell. However, the prediction is structurally consistent with the unit cell of BTR that was determined by single crystal diffraction.³ If one assumes BQR adopts similar crystal packing to BTR, then there should only be a shift in the crystal dimension in the direction parallel to the molecular backbone; recall that BQR is identical to BTR except for the addition of a thiophene on either side of the benzodithiophene core. The molecular backbone of BTR is orthogonal to the *b*-axis of the unit cell and effectively coincident with the <201> direction (Figure S7). Thus, the length of a BXR molecule with the structural motif of BTR can be estimated from

the lattice constants: $l_{BXR} \approx \sqrt{(2a)^2 + c^2 - (2ac)\cos(\beta)}$. With the addition of two thiophene units, $\approx 4\text{\AA}$ in length each, one expects $l_{BQR} \approx l_{BTR} + 8\text{\AA}$. Directly computing these lengths from the unit cell parameters, $l_{BTR} \approx 38\text{\AA}$ and $l_{BQR} \approx 51\text{\AA}$. Accounting for thermal expansion in the BQR crystal at $150\text{ }^\circ\text{C}$ in the GIWAXS sample compared to the BTR single crystal analyzed at $-173\text{ }^\circ\text{C}$ the difference in lengths (13\AA) is entirely consistent with molecular intuition. However, we note that the GIXD estimate is not a replacement for single crystal measurements and errors on the order of several percent can be expected.

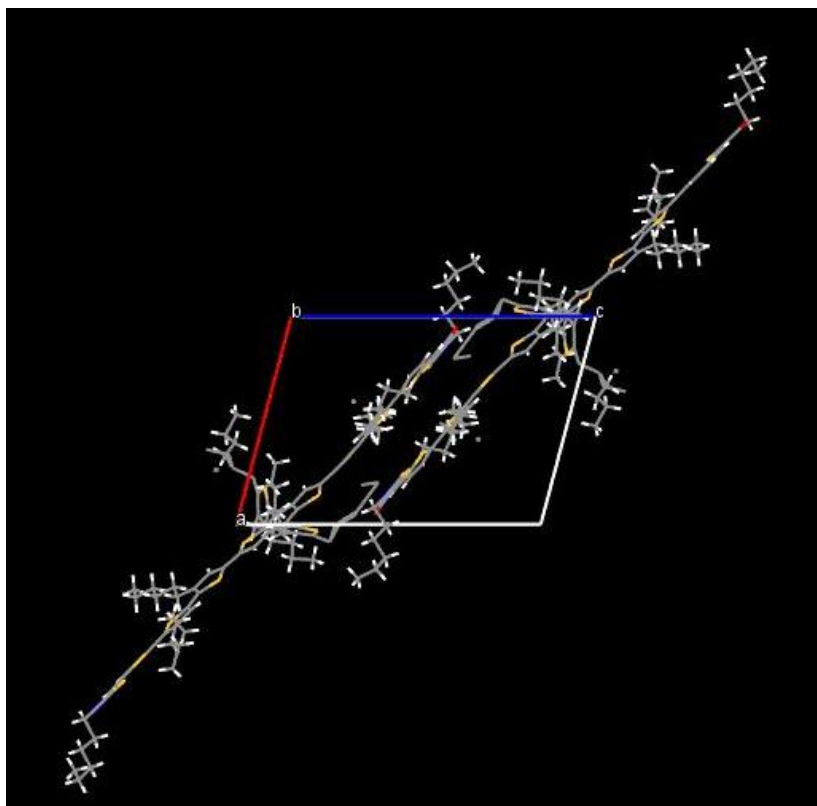


Figure S7. View down the *b*-axis of BTR.

References

- (1) Hailey, A. K.; Hiszpanski, A. M.; Smilgies, D.-M.; Loo, Y.-L. The Diffraction Pattern Calculator (DPC) Toolkit: A User-Friendly Approach to Unit-Cell Lattice Parameter Identification of Two-Dimensional Grazing-Incidence Wide-Angle X-Ray Scattering Data. *J. Appl. Crystallogr.* **2014**, *47* (Pt 6), 2090–2099.
- (2) Müller-Buschbaum, P. The Active Layer Morphology of Organic Solar Cells Probed with Grazing Incidence Scattering Techniques. *Adv. Mater.* **2014**, *26* (46), 7692–7709.
- (3) Sun, K.; Xiao, Z.; Lu, S.; Zajackowski, W.; Pisula, W.; Hanssen, E.; White, J. M.; Williamson, R. M.; Subbiah, J.; Ouyang, J.; et al. A Molecular Nematic Liquid Crystalline Material for High-Performance Organic Photovoltaics. *Nat. Commun.* **2015**, *6* (1), 6013.